Recognition in Excitable Chemical Reactor Networks. Experiments and Model-Simulations

W. Hohmann, M. Kraus, and F. W. Schneider*

Institute of Physical Chemistry, University of Würzburg, Am Hubland, 97074 Würzburg, Germany

Received: June 13, 1997; In Final Form: July 18, 1997[⊗]

A reactor network consisting of four electrically coupled Belousov−Zhabotinsky (BZ) oscillators is used for the recognition of chemical oscillation patterns. The four reactors show identical period-1 oscillations. The application of a constant electrical current drives the period-1 oscillations into an excitable nodal steady state via a saddle-node infinite period (SNIPER) bifurcation. Global electric coupling is achieved by periodic external pulses applied simultaneously to all four nodal steady states. Thus, any two of eight possible oscillation patterns can be established as initial conditions. Local electrical coupling according to a programming rule enables the network to carry out the actual recognition process of the two encoded patterns. As a result, the two encoded patterns are immediately selected if offered as initial conditions. A pattern with one error is corrected within one or two oscillations; however, patterns with two errors are rejected by this experimental network. Numerical simulations with the seven-variable Györgyi−Field model of the BZ reaction, which is perturbed by a flow of electrical charge, are in good agreement with the experimental results. The advantages of "fast" electrical coupling over "slow" mass coupling are discussed.

Introduction

The coupling of chemical reactors by mass exchange[1,2] and by electric currents[3] has been the subject of several studies owing to its analogy to biological systems. The Boolean functions were implemented experimentally by flow rate coupling of three chemical reactors using the bistable minimal bromate system[4] and the monostable neutralization reaction.[5] Theoretical studies on the implementation of logic functions were made by Hjelmfelt et al.[6] and Lebender et al.[7] Mass coupling of two excitable chemical reactors was initially carried out by Marek and co-workers[8] who studied the effects of stimulus propagation in the two reactors. Based on theoretical considerations,[9] pattern recognition by mass coupling was performed by Laplante et al.[10] for the first time who used a mass-coupled eight-reactor network containing the bistable iodate−arseneous acid reaction.

In previous work[11] electrical rather than mass coupling among four chemical reactors was employed in order to encode and recognize oscillation patterns obtained from periodic perturbations of an excitable focus in the Belousov−Zhabotinsky (BZ) reaction. Electrical coupling turned out to be very efficient and more rapid than mass coupling. The four-reactor network was coupled via Pt working electrodes[11] whose individual potentials depended on the potentials of the neighboring reactors in a defined way. Thus, all four reactors were initially run in a focal steady state that changed into a limit cycle when the value of the bifurcation parameter was moved across a Hopf bifurcation. The bifurcation parameter consisted of an externally applied potential. This potential was varied periodically and all four reactors showed in-phase forced oscillations. In addition to the latter global coupling procedure, a local coupling interaction was activated according to a Hopfield matrix[12] in order to initiate the recognition process. Hopfield networks[12] are able to recognize encoded patterns even if the presented patterns contain errors with respect to the encoded patterns. Two (out of eight possible) oscillation patterns were encoded in the network by time-delayed feedback according to Pyragas,[13] which made it possible to achieve a 180° phase shift between two oscillations. Since the starting pattern was always a "homogeneous" pattern (i.e., all four reactors were in phase), the recognition process consisted of obtaining a 50:50 distribution of the two encoded patterns in many experiments.

To achieve the unique recognition of any of the two encoded patterns (and not a 50:50 distribution of the two encoded patterns), we follow a different strategy in the present experiments. Instead of a focal steady state, we use a P1 state of the BZ reaction, since we discovered that the application of an electric current to the P1 state will lead to a *nodal* steady state via a saddle-node infinite period bifurcation (SNIPER). A nodal steady state that is reached via a SNIPER bifurcation is excitable,[14] i.e., a single pulse perturbation across the SNIPER bifurcation will produce a single large amplitude response of the chemical reaction resembling an action potential in the present system. A subsequent pulse perturbation will be effective only after the refractory time has passed. When the perturbation is applied in a periodic fashion by turning the electric current off and on, the SNIPER bifurcation is crossed periodically from the nodal steady state to the period-one state. This procedure generates a doubled response period (1:2 response) over a sufficiently wide frequency range, which makes it possible to generate and stabilize any one of eight ($2^4/2$) possible firing patterns as initial patterns. Although this global coupling term is always present to stabilize any chosen initial pattern, local coupling is turned on subsequently in order to carry out the actual recognition process. In contrast to our previous work, we use in-phase coupling without any delay time as shown by the positive entries in the Hopfield matrix.

Experimental Section

The experimental setup (Figure 1) consists of four continous flow stirred tank reactors (CSTRs) where each CSTR (4.2 mL volume, 25.0 °C) is connected to its own reference chamber via a Teflon membrane. Each CSTR contains a monitoring Pt/Ag/AgCl redox electrode together with a Pt working electrode that delivers the electrical current, a stirrer (600 rpm), three tubes for the inflow of reactant solutions, and an outflow tube. The reference chamber acts as a reference half cell containing 0.4 mol/L sulfuric acid without any stirring. In principle, any

[⊗] Abstract published in *Advance ACS Abstracts,* September 1, 1997.

S1089-5639(97)01939-7 CCC: $14.00 © 1997 American Chemical Society

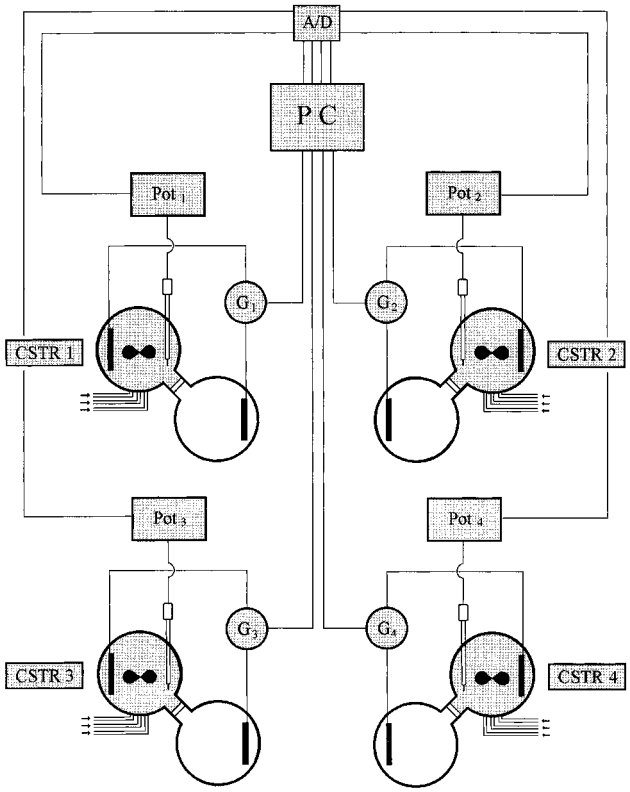

Figure 1. Four CSTRs are each connected to its own reference chamber by a membrane. The redox potentials Pot_i are monitored by Pt/Ag/AgCl redox electrodes. Electrical currents G_i (eq 2) are applied to Pt working electrodes inserted in each reactor.

number of CSTR/reference reactor pairs can be used to build up an electrically coupled reactor network. The reactant solutions are contained in three 50 mL glass syringes per reactor where a precise piston pump delivers the reactant solutions into the CSTR at any prescribed flow rate. To establish a P1 BZ state, the following reactant solutions were used: syringe I, 0.42 mol/L $KBrO_3$; syringe II, 1.5×10^{-3} mol/L $Ce_2(SO_4)_3$ and 0.9 mol/L malonic acid (Merck); syringe III, 1.125 mol/L sulfuric acid. The slight difference in the sulfuric acid concentrations between the reference cell (0.4 mol/L) and the BZ cell (0.375 mol/L) is not of any significance. All reagents are of the highest available purity. Owing to variations in the sensitivities of the redox electrodes, their potentials are presented in arbitrary units. At the start of each recognition experiment the electrode potentials are adjusted to 1000 units before local coupling is initiated. All redox potentials are recorded digitally in 1 s intervals. Four galvanostats (E&G Instruments) deliver the electric current to the Pt working electrodes according to eq 2.

SNIPER Bifurcation. In the absence of an electrical current the bifurcation diagram given in Figure 2 has been determined in a single CSTR for the above reactant concentrations. Period-1 oscillations (P1) prevail over a large region of the flow rate from $k_f \approx 2.5 \times 10^{-4}$ s^{-1} to $\sim 10.0 \times 10^{-4}$ s^{-1}. Hopf bifurcations occur at $k_f = 2.5 \times 10^{-4}$ s^{-1} (HB_1), $k_f = 12.0 \times 10^{-4}$ s^{-1} (secondary Hopf bifurcation HB_2), and $k_f = 12.5 \times 10^{-4}$ s^{-1} (HB_3) with focal steady states SS_1 und SS_2. Mixed mode oscillations occur in the Farey region. For the coupling experiments the flow rates in each reactor were identical and constant at $k_f = 6.0 \times 10^{-4}$ s^{-1}.

For increasing cathodic currents the frequency of the P1 oscillations is observed to decrease to zero (Figure 3a) at a bifurcation point that is typical of a saddle-node infinite period (SNIPER) bifurcation.[14] This indicates that a limit cycle (P1) collides with a saddle node at the bifurcation point, leading to

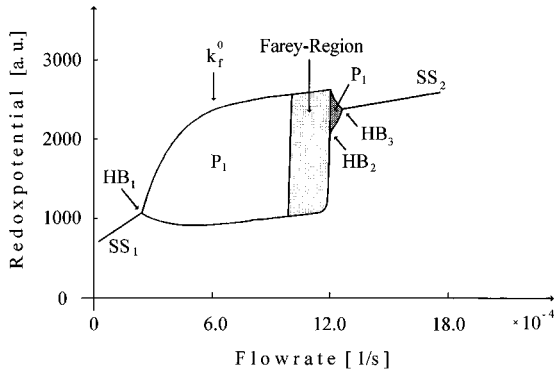

Figure 2. Experimental bifurcation diagram of the free running BZ reaction: (P1) oscillations of period-1; (HB_1, HB_3) supercritical Hopf bifurcations; (HB_2) secondary Hopf bifurcation; (SS_1, SS_2) focal steady states; (k_f^o) flow rate used in the coupling experiments.

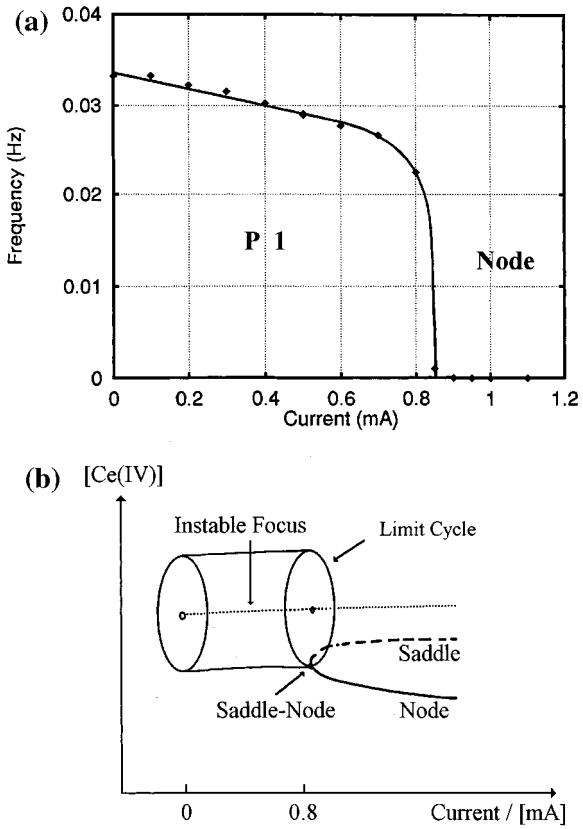

Figure 3. (a) Experimentally obtained SNIPER bifurcation using the electric current as bifurcation parameter. The frequency of P1 oscillations decreases to zero for an increasing electric current. (b) SNIPER bifurcation. A saddle-node collides with a limit cycle, leading to oscillations of infinite period at the bifurcation point. The amplitude of the experimental limit cycle remains almost constant from 0 to 0.85 mA.

oscillations of "infinite" period (Figure 3b). This interesting bifurcation has not yet been reported so far for an electrical current as the bifurcation parameter. When the cathodic current is further increased beyond 0.85 mA (SNIPER bifurcation), a nodal steady state is reached. This nodal steady state is excitable as evidenced by a large amplitude excursion when it is perturbed across the SNIPER bifurcation by a sudden reduction of the electric current below 0.85 mA followed by a subsequent increase above 0.85 mA. The excitability of the nodal steady state is used in the following coupling experiments to recognize firing patterns by the reactor network.

Global Coupling. Owing to the nonlinearity of the BZ reaction an electric rectangular pulse train applied to a P1 free

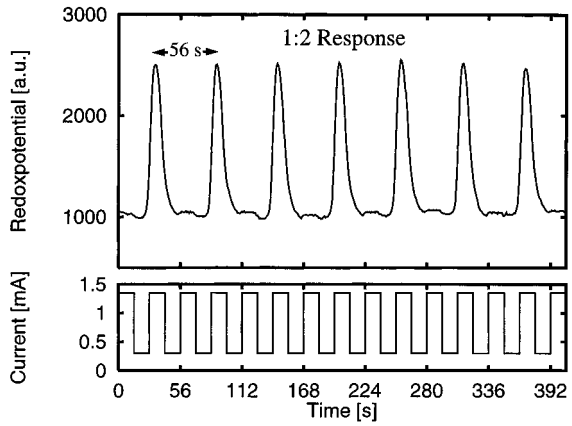

Figure 4. Global coupling and 1:2 response. Characteristics of the periodic forcing current are $I_{max} = 1.35$ mA, $I_{min} = 0.25$ mA, pulse length = 14 s, forcing period = 28 s, and response period $T = 56$ s.

running oscillatory state leads to a 1:2 response of the system for sufficiently high-current amplitudes as shown in Figure 4, where $I_{max} = 1.35$ mA (nodal steady state), $I_{min} = 0.25$ mA (P1 state), pulse length is 14 s, and the forcing period is 28 s. The period of the forced response turns out to be twice the forcing period, namely, 56 s, indicating that the refractory time is between 28 s (perturbation period) and 56 s (1:2 response period). For two electrically coupled P1 oscillators the response oscillations may be stabilized either in phase or out of phase. Thus, for the present four-reactor network, eight ($2^4/2$) different oscillation patters (firing patterns) are possible if all four coupled reactors are driven simultaneously by the same electrical pulse train (Figure 5). This periodic driving across the SNIPER bifurcation leads to forced oscillations in all four reactors, a procedure that we call *global* coupling. It will be seen that recognition of a specific initial oscillation pattern is not possible without global coupling in the present network.

Local Coupling and the Hopfield Network. Additional coupling between the individual reactors will be called *local* coupling. The choice of the encoded patterns for the recognition process will determine the particular connectivities for local coupling. A very useful representation of local coupling is provided by the Hopfield matrix[12] in which the entries (rows and columns) represent the coupling strengths between two coupled reactors. In the Hopfield matrix the coupling strengths w_{ij} between reactor i and j are calculated according to eqs 1 where p is the number of patterns to be encoded and stored in the network:

$$w_{ij} = \sum_{1}^{P} x_i x_j \quad \text{for} \quad i \neq j$$

$$w_{ij} = 0 \quad \text{for} \quad i = j \tag{1}$$

where the product of the statistical weights x_i and x_j for in-phase coupling and out-of-phase coupling is $+1$ and -1, respectively. The statistical weights may be presented in the Hopfield matrix **W** for encoded patterns 1 and 2 (Figure 5) as follows (for $p = 2$):

$$\mathbf{W} = \begin{pmatrix} 0 & 2 & 0 & 2 \\ 2 & 0 & 0 & 2 \\ 0 & 0 & 0 & 0 \\ 2 & 2 & 0 & 0 \end{pmatrix}$$

For the encoded patterns 1 and 2 this bipolar notation leads to a symmetric matrix with positive entries (between reactors 1 and 2, 1 and 4, 2 and 4) and entries of zero (between reactors 1 and 3, 2 and 3, 3 and 4), since reactor 3 is not locally (but globally) coupled with the other reactors. In our previous recognition experiments[11] different patterns were stored in a four-reactor network where out-of-phase local coupling had to be used between two reactor pairs. The latter procedure lead to a Hopfield matrix with negative entries according to eqs 1 and 2, indicating out-of-phase coupling.

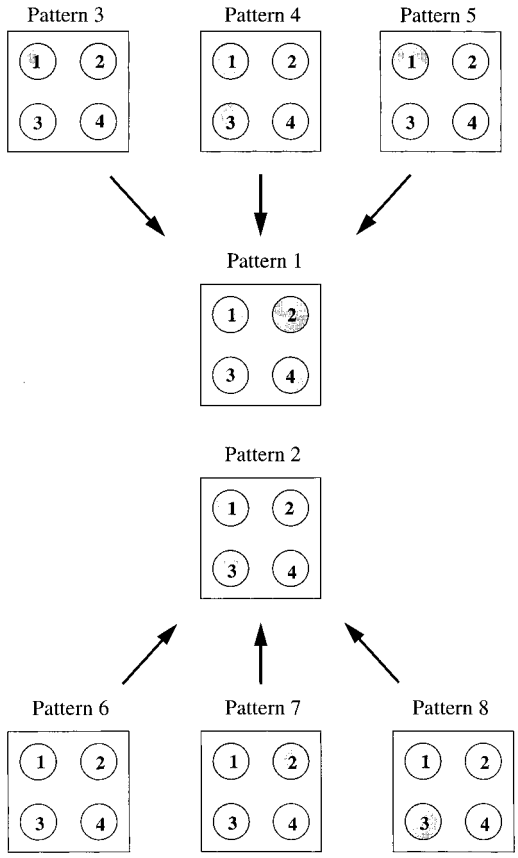

Figure 5. Eight possible oscillation patterns. Patterns 1 and 2 are encoded; patterns 3−5 (6−8) have one error with respect to pattern 1 (pattern 2) and two errors with respect to pattern 2 (pattern 1). Dark circles indicate oscillation maximum, and light circles indicate oscillation minimum. The numbers in the circles refer to reactors.

Encoding Two of Eight Firing Patterns. All eight possible oscillation (firing) patterns in a four-reactor network are shown in Figure 5, where a dark circle represents a maximum in an oscillation and a light circle represents a minimum (or vice versa). There are eight mirror images, i.e., patterns in which the oscillation maxima of the above patterns are shifted by 180° to become minima. They are excluded here, since they are equivalent to the above eight patterns. For the recognition experiments we have selected two patterns (out of eight patterns) to be stored (encoded) in the network, i.e., six out of eight are unknown (untrained) patterns. Inspection of patterns 3−5 (6−8) shows that they bear one error with respect to pattern 1 (2) and two errors relative to pattern 2 (1). We have selected the two patterns in order to achieve a unique recognition of an encoded pattern and not a 50:50 distribution of the two encoded patterns as in previous work.[11]

Local coupling is implemented experimentally by using four galvanostats where each galvanostat provides the current for the working Pt electrode in the respective reactor (G_1−G_4). The individual G_i values are calculated by a computer from the instantaneous potentials in the other coupled reactors as

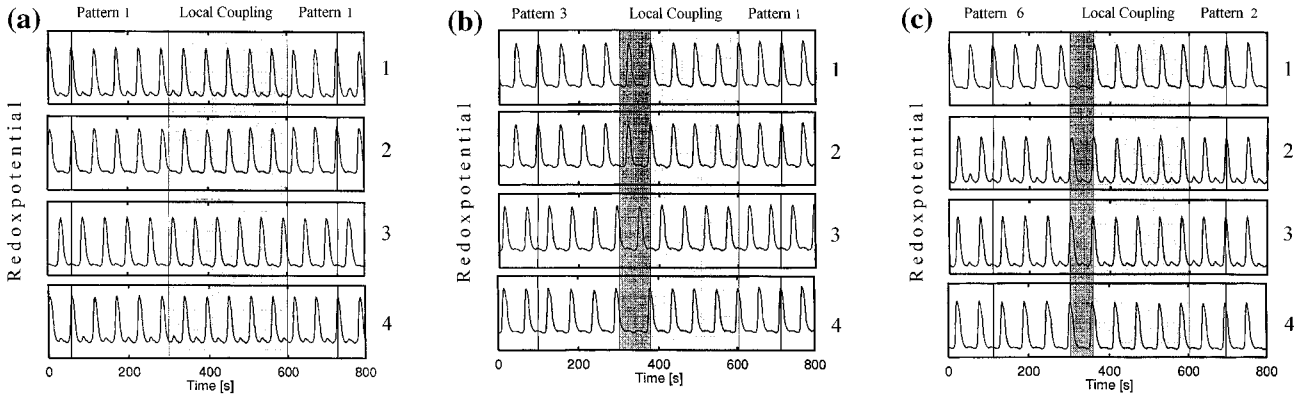

Figure 6. Experimental time series of recognition processes using (a) pattern 1, (b) pattern 3, and (c) pattern 6 as initial patterns. The shaded area indicates the presence of local coupling, while the dark shaded areas indicate the approximate transient time. In part a the encoded pattern 1 is preserved. In parts b and c pattern 3 (pattern 6) is recognized as pattern 1 (pattern 2). One error is tolerated and corrected.

measured by a conventional redox electrode in each reactor. Global coupling consists of a forcing periodic pulse train (Figure 4).

The coupling scheme for simultaneously encoding patterns 1 and 2 may also be diplayed as

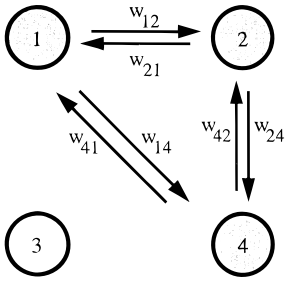

where

$$G_1(t) = \text{global coupling} + w_{21}\{\text{Pot}_2(t) - \text{Pot}_1(t)\} + w_{41}\{\text{Pot}_4(t) - \text{Pot}_1(t)\}$$

$$G_2(t) = \text{global coupling} + w_{12}\{\text{Pot}_1(t) - \text{Pot}_2(t)\} + w_{42}\{\text{Pot}_4(t) - \text{Pot}_2(t)\}$$

$$G_3(t) = \text{global coupling} + 0$$

$$G_4(t) = \text{global coupling} + w_{14}\{\text{Pot}_1(t) - \text{Pot}_4(t)\} + w_{24}\{\text{Pot}_2(t) - \text{Pot}_4(t)\} \quad (2)$$

All nonzero w_{ij} are set equal. $\text{Pot}_i(t)$ is the redox potential in reactor i. The coupling functions $G_i(t)$ are small electric currents with global coupling between 0.25 and 1.35 mA. The w_{ij} were chosen such that the contribution of local coupling was maximally 0.5 mA, i.e., $w_{ij} = 0.25$ μA for optimal local coupling, where the difference in the potentials was maximally 1000 arbitrary units. This causes two electrically coupled reactors i and j to oscillate in phase. Thus, after local coupling has been activated, reactors 1 and 2, 1 and 4, and 2 and 4 will oscillate in phase, i.e., there are three "reversible" couplings in this four-reactor network. Since reactor three is locally uncoupled, its phase will depend entirely on its initial condition, which will be preserved throughout an experiment because of the stabilizing effect of global coupling.

Results

Experiments. The flow rate in all experiments was fixed at $k_f^\circ = 6.0 \times 10^{-4}$ s^{-1} corresponding to a residence time of 27.8 min. This relatively long residence time provides a ~15 h duration for a single experiment, i.e., for a single filling of the syringes. The same nodal steady state is established in each reactor by the application of an identical electrical current. Conversion due to redox processes at the working electrode is kept relatively small, amounting to less than 10% of the Ce^{4+} concentration due to the chemical reaction.

Initial Conditions. Any of the eight possible initial patterns may be established experimentally with equal probability for each pattern (Figure 5). A given initial pattern is prepared either through small electrical perturbations or by the addition of a small amount of Ce^{4+} solution according to the phase-resetting curve as determined earlier.[15] If unperturbed, an initial pattern remains stable indefinitely in all experiments shown in this work. Next, the activation of local coupling initiates the recognition process according to eq 2. For an insufficient local coupling strength the given initial pattern remains unperturbed. At the optimal coupling strength w_{ij} the recognition process is finished in less than 100 s for all initial patterns, i.e., in less than two oscillations. Figure 6 shows three exemplary time series describing the recognition process, where local coupling has been activated at the 300 s mark. When local coupling is turned off arbitrarily at the 600 s mark, the selected patterns remain indefinitely because of the sustained presence of global coupling. When one of the encoded oscillation patterns is chosen as an initial pattern (such as pattern 1 in Figure 6a), recognition is achieved immediately, since the contribution of local coupling to $G_i(t)$ is negligible from the start. In other words, there are no errors to be corrected here and global coupling is the only contribution to the $G_i(t)$ currents. For the recognition of pattern 1 starting with an initial pattern having one error (or two errors relative to pattern 2) we show a representative time series using pattern 3 as the initial pattern (Figure 6b). The selected pattern 1 is recognized in less than 100 s (corresponding to less than two oscillations) as seen by the dark shaded area. In this recognition experiment, reactor 4 receives two simultaneous signals from reactors 1 and 2 (eq 2). Thus, the large total signal due to local coupling forces reactor 4 into the same phases as reactors 1 and 2. Patterns 4 and 5 are recognized (not shown) with the same efficiency as pattern 3. The remaining patterns 6−8 contain one error with respect to pattern 2 and two errors with respect to pattern 1. In recognition experiments the pattern with the smallest number of errors is always selected. As an example, we show pattern 6 as the initial pattern (Figure 6c). After a transient time of only one oscillation period, pattern 2 has been selected by the electrically coupled reactor network. Similarly, patterns 7 and 8 change into pattern 2 (not shown) with the same efficiency as pattern 6 does.

TABLE 1: Seven-Variables Model (Nonstoichiometric Steps)[a]

$Br^- + HBrO_2 + H^+$	→	2BrMA	(R1)
$Br^- + BrO_3^- + 2H^+$	→	$BrMA + HBrO_2$	(R2)
$2HBrO_2$	→	$BrO_3^- + BrMA + H^+$	(R3)
$BrO_3^- + HBrO_2 + H^+$	→	$2BrO_2^\bullet + H_2O$	(R4)
$2BrO_2^\bullet + H_2O$	→	$BrO_3^- + HBrO_2 + H^+$	(R5)
$Ce^{3+} + BrO_2^\bullet + H^+$	→	$HBrO_2 + Ce^{4+}$	(R6)
$HBrO_2 + Ce^{4+}$	→	$Ce^{3+} + BrO_2^\bullet + H$	(R7)
$MA + Ce^{4+}$	→	$MA^\bullet + Ce^{3+} + H^+$	(R8)
$BrMA + Ce^{4+}$	→	$Ce^{3+} + Br^-$	(R9)
$Ma^\bullet + BrMA$	→	$MA + Br^-$	(R10)
$2MA^\bullet$	→	MA	(R11)

[a] MA = malonic acid. MA• = malonic acid radical. BrMA = bromomalonic acid.

TABLE 2: Rate Constants and Concentrations of the Seven-Variables Model

k_{R1}	$2.0 \times 10^6\ s^{-1}\ M^{-2}$	k_{R2}	$2.0\ s^{-1}\ M^{-3}$
k_{R3}	$3.0 \times 10^3\ s^{-1}\ M^{-2}$	k_{R4}	$3.3 \times 10^1\ s^{-1}\ M^{-2}$
k_{R5}	$7.6 \times 10^5\ s^{-1}\ M^{-2}$	k_{R6}	$6.2 \times 10^4\ s^{-1}\ M^{-2}$
k_{R7}	$7.0 \times 10^3\ s^{-1}\ M^{-2}$	k_{R8}	$3.0 \times 10^{-1}\ s^{-1}\ M^{-1}$
k_{R9}	$3.0 \times 10^1\ s^{-1}\ M^{-2}$	k_{R10}	$2.4 \times 10^4\ s^{-1}\ M^{-2}$
k_{R11}	$3.0 \times 10^9\ s^{-1}\ M^{-2}$		
$[BrO_3^-]$	0.1 M	$[H^+]$	0.26 M
$[H_2O]$	55 M	$[Ce^{3+}]_0$	8.33×10^{-4} M
[MA]	0.25 M		

At excessively high coupling strengths the phases of the oscillators start to drift, indicating nonrecognition (not shown).

Simulations. **Model of the Nonlinear Seven-Variables Montanator**. In analogy to our experiments we use computer simulations to simulate pattern recognition with the seven-variables montanator model,[16] which was developed by Györgyi and Field. The model consists of two autocatalytic cycles, one describing the production of $HBrO_2$ by the reduction of bromate with Ce^{3+} and the other the formation of Br^- from bromomalonic acid as an autocatalytic species. The mechanism of the seven-variables montanator is given in Table 1, the rate constants and concentrations of the inflow species in Table 2. The variables are bromous acid, bromide, bromate, bromomalonic acid, bromomalonic acid radical, Ce^{3+}, and Ce^{4+}. The numerical integrations of the differential equations were performed using the Gear method.[17] A bifurcation diagram with the electric current C as the bifurcation parameter is given in Figure 7a, where the flow rate was kept constant at $k_f = 3.5 \times 10^{-4}\ s^{-1}$.

The effect of the electric current enters into the differential equations by adding $+C[Ce^{4+}]$ to the rate equation for $[Ce^{3+}]$ and by adding the negative term $-C[Ce^{4+}]$ to the rate equation of $[Ce^{4+}]$:

$$\frac{d[Ce^{3+}]}{dt} = f([Ce^{3+}]) - k_f([Ce^{3+}]) - [Ce^{3+}]_0 + C[Ce^{4+}]$$

$$\frac{d[Ce^{4+}]}{dt} = f([Ce^{4+}]) - k_f([Ce^{4+}]) - C[Ce^{4+}]$$

where C is a rate parameter proportional to the amount of charge delivered at the Pt working electrode, $[Ce^{3+}]_0$ is the inflow concentration of Ce^{3+} (Table 2), and $f([Ce^{3+}])$ contains the respective rate equation characteristic of the model (Table 1).

P1 oscillations exist between $C = 0$ and $0.10\ s^{-1}$. In analogy to the experiments a SNIPER bifurcation exists (at $C = 0.11\ s^{-1}$) beyond which a nodal steady state is observed. The frequency of the P1 oscillations is plotted versus the electric current in Figure 7b. The frequency of the P1 oscillations

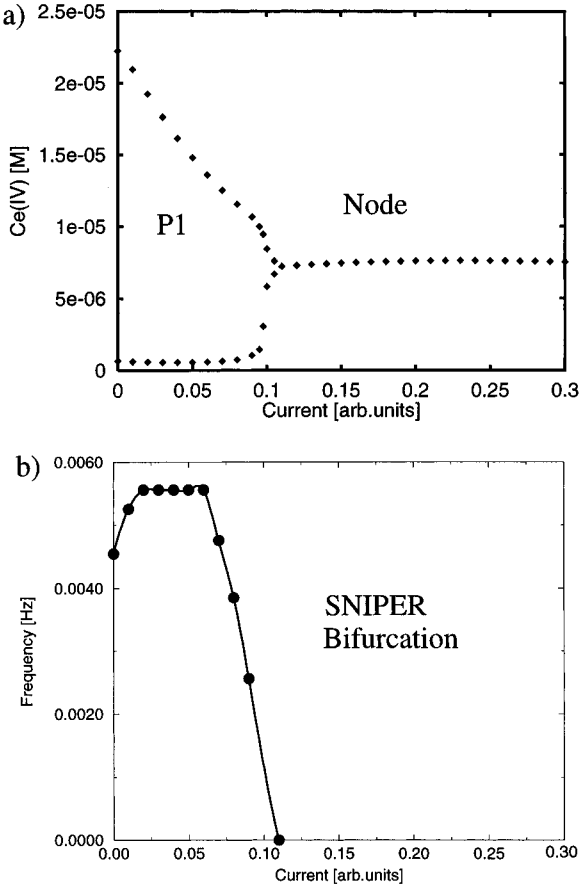

Figure 7. Bifurcation diagram of the model (Table 1) simulations using the electric current as a bifurcation parameter. Part a shows $[Ce^{4+}]$ versus current. At a current of 0.10 the P1 oscillations change into a node where the amplitude of the calculated P1 limit cycle has decreased to zero. Part b shows the frequency of P1 oscillations versus current. At the bifurcation point the frequency decreases to zero, indicating a SNIPER bifurcation in analogy to the experiment results.

declines from $4.76 \times 10^{-3}\ s^{-1}$ at $C = 0.07\ s^{-1}$ to zero at $C = 0.11\ s^{-1}$, which is typical of a SNIPER bifurcation (Figure 7b). In analogy to the experiments we used each of the eight possible oscillation patterns as initial conditions in the simulations under global coupling. Subsequently, local coupling was turned on at the 1000 s mark (Figure 8). Recognition of the nonencoded patterns occurred in a similar fashion as in the experiments. The calculated oscillations showed a small shoulder, which is observed in the experiments as a small peak between two large peaks. This effect is attributed to a second pulse that arrives during the refractory time of the first peak. Thus, the effect of the second pulse is almost completely suppressed. Therefore, in the simulations, the value of the refractory time is between the perturbation period and the response period as in the experiments. The transient time observed for the recognition process is about twice as long (about four oscillations) in the simulations as in the experiments, which is believed to be due to the choice of the particular theoretical model.

Discussion

Crossing a SNIPER bifurcation (between a limit cycle and a *nodal* steady state) with the electric current as a bifurcation parameter proves to be the most rapid method yet for pattern recognition in a nonlinear chemical reactor network. It is superior in speed to our previous recognition experiments, which electrically perturbed a *focal* BZ state to cross a Hopf bifurcation. Most importantly, the presence of the SNIPER bifurcation

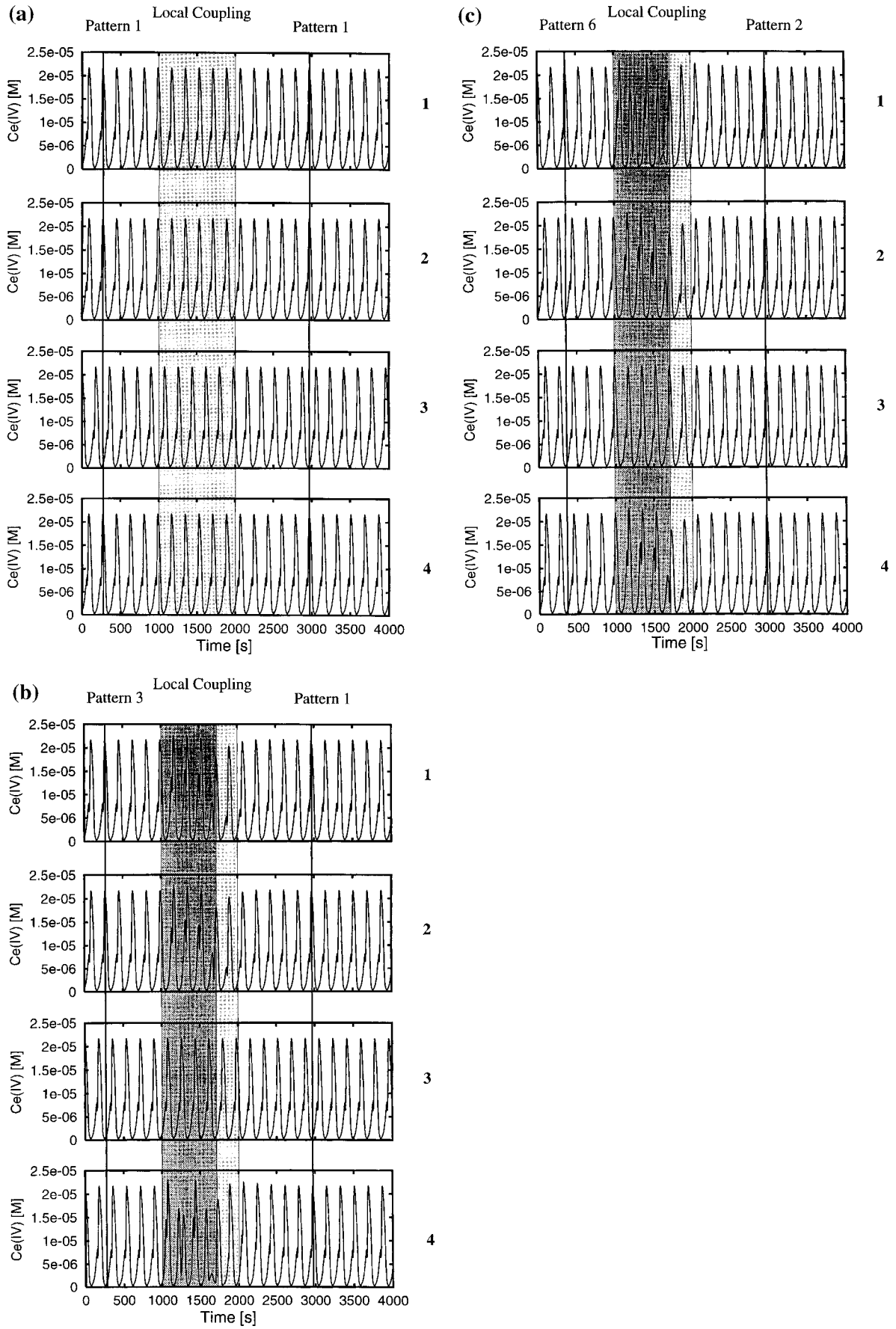

Figure 8. Model simulations. Part a shows the time series of recognition processes (same as Figure 6). Transient times in parts b and c are about twice as long (about four 4 oscillations) as in Figure 6.

allows any of the eight possible firing patterns to be easily prepared as a stable initial pattern because of the 1:2 response of the reaction to global coupling. All initial patterns are equally stable. This is in contrast to our previous experiments,[11] which

applied a periodic current to a focal steady state of the BZ reaction where a 1:1 instead of a 1:2 response was obtained for global coupling. Therefore, our previous work[11] only allowed one set of initial conditions, namely, all four reactors being in synchrony (in phase).

In the present experiments, only phase shifts of 0° or 180° are observed owing to the 1:2 ratio of the perturbation period and the response period. Arbitrary phase shifts cannot be stabilized here, which indicates that information may not be encoded in the phase angles. Furthermore, the relatively large experimental fluctuations in the phases would obscure any small phase shifts.

When any two reactors of reactors 1, 2, or 4 are in identical states, the third reactor will be driven into the same state according to eq 2 owing to a doubled local signal that is contributed by the other two reactors. A single contributing signal will not be sufficient to cause a 180° phase shift. This simple situation is at the heart of the recognition process, and it guarantees its uniqueness. Once all three reactors are in identical states, the contributions of local coupling to the signals $G_1(t)$, $G_2(t)$, and $G_4(t)$ approach zero (except for the periodic signal due to global coupling) and further changes in a pattern no longer occur. From the two encoded patterns, the one with the least number of errors relative to a chosen initial pattern is recognized and selected by the network. For the present four-reactor network there are either zero, one, or two errors; however, the recognition process never selects an encoded pattern that shows 2 possible errors with respect to the initial pattern.

In all experiments the coupling constants w_{ij} were experimentally adjusted for optimal operation and set equal. Variations in the w_{ij} values may be introduced in larger networks.

Comparison with Mass Coupling. Pattern recognition has been performed experimentally for the first time by Laplante, Pemberton, Hjelmfelt, and Ross (LPHR)[10] who used a network of eight mass-coupled chemical reactors containing the bistable iodate−arseneous acid reaction. A limited number of patterns could be recognized only (for a short discussion see ref 11). Mass coupling is experimentally demanding, since all reactors have to be necessarily in close proximity. Furthermore, negative entries in the Hopfield matrix cannot be realized by mass coupling. On the other hand, electrical coupling does not require proximity of the reactors; the coupled reactor/reference pairs could be located simultaneously on different continents, for example. The speed of the recognition process is necessarily faster in electrical coupling, since the rates of the redox processes at the Pt working electrodes are at least an order of magnitude faster than any effective mass exchange rates.

Comparison with Neural Nets. Reactor networks may be viewed as generic models for small neural nets, since electrical coupling and excitable steady states also occur in biological neurons. In the present work the excitable nodal steady state is analogous to the "polarized" state of a neuron whereas the free running limit cycle may represent the "depolarized" state. Activation of a reactor is achieved by an applied electric current to produce an excitable nodal steady state. Inhibition may be viewed as an additional application of an electrical current, which will hardly affect an already established nodal state. It is possible to design a reactor network that includes learning processes according to a Hebbian rule.

Acknowledgment. We thank the Deutsche Forschungsgemeinschaft and the Fonds der Chemischen Industrie for financial support of this work.

References and Notes

(1) Marek, M.; Stuchl, I. *Biophys. Chem.* **1975**, *3*, 241. Nakajima, K.; Sawada, Y. *J. Chem. Phys.* **1980**, *72*, 2231. Stuchl, I.; Marek, M. *J. Chem. Phys.* **1982**, *77*, 1607. Bar-Eli, K. *J. Phys. Chem.* **1984**, *88*, 3616. Bar-Eli, K.; Reuveni, S. *J. Phys. Chem.* **1985**, *89*, 1329. Boukalouch, M.; Elezgaray, J.; Arneodo, A.; Boissonade, J.; De Kepper, P. *J. Phys. Chem.* **1987**, *91*, 5843. Crowley, M. F.; Epstein, I. R. *J. Phys. Chem.* **1989**, *93*, 2496. Yoshimoto, M.; Yoshikawa, K.; Mori, Y.; Hanazaki, I. *Chem. Phys. Lett.* **1992**, *189*, 18. Laplante, J.-P.; Erneux, T. *J. Phys. Chem.* **1992**, *96*, 4931. Doumbouya, S. I.; Münster, A. F.; Doona, C. J.; Schneider, F. W. *J. Phys. Chem.* **1993**, *97*, 1025. Doumbouya, S. I.; Schneider, F. W. *J. Phys. Chem.* **1993**, *97*, 6945. Hauser, M. J. B.; Schneider, F. W. *J. Chem. Phys.* **1994**, *100*, 1058. Booth, V.; Erneux, T.; Laplante, J.-P. *J. Phys. Chem.* **1994**, *98*, 6537.

(2) Zhabotinskii, A. M.; Zaikin, A. N.; Rovinskii, A. B. *React. Kinet. Catal. Lett.* **1982**, *20*, 29. Weiner, J.; Schneider, F. W.; Bar-Eli, K. *J. Phys. Chem.* **1989**, *93*, 2704. Chevalier, T.; Freund, A.; Ross, J. *J. Chem. Phys.* **1991**, *95*, 308. Roesky, P. W.; Doumbouya, S. I.; Schneider, F. W. *J. Phys. Chem.* **1993**, *97*, 398. Weiner, J.; Holz, R.; Schneider, F. W.; Bar-Eli, K. *J. Phys. Chem.* **1992**, *96*, 8915. Holz, R.; Schneider, F. W. *J. Phys. Chem.* **1993**, *97*, 12239. Zeyer, K.-P.; Holz, R.; Schneider, F. W. *Ber. Bunsen-Ges. Phys. Chem.* **1993**, *97*, 1112.

(3) Crowley, M. F.; Field, R. J. In *Nonlinear Phenomena in Chemical Dynamics*; Vidal, C., Pacault, A., Eds.; Springer: Berlin, 1981; p 147. Crowley, M. F.; Field, R. J. In *Lecture Notes in Biomathematics, Nonlinear Oscillations in Biology and Chemistry*; Othmer, H., Ed.; Springer: Berlin; 1986; p 68. Crowley, M. F.; Field, R. J. *J. Phys. Chem.* **1986**, *90*, 1907. Botré, C.; Lucarini, C.; Memoli, A.; D'Ascenzo, E. *Bioelectrochem. Bioenerg.* **1981**, *8*, 201. Schneider, F. W.; Hauser, M. J. B.; Reising, J. *Ber. Bunsen-Ges. Phys. Chem.* **1993**, *97*, 55. Zeyer, K.-P.; Münster, A. F.; Hauser, M. J. B; Schneider, F. W. *J. Chem. Phys.* **1994**, *101*, 5126.

(4) Zeyer, K.-P.; Dechert, G.; Hohmann, W.; Blittersdorf, R.; Schneider, F. W. *Z. Naturforsch.* **1994**, *49A*, 953.

(5) Blittersdorf, R.; Müller, J.; Schneider, F. W. *J. Chem. Educ.* **1995**, *72*, 760.

(6) Hjelmfelt, A.; Weinberger, E. D.; Ross, J. *Proc. Natl. Acad. Sci. U.S.A.* **1991**, *88*, 10983; *Proc. Natl. Acad. Sci. U.S.A.* **1992**, *89*, 383.

(7) Lebender, D.; Schneider, F. W. *J. Phys. Chem.* **1994**, *98*, 7533.

(8) Kosek, J.; Marek, M. *J. Phys. Chem.* **1993**, *97*, 120. Dolník, M.; Kosek, J.; Votrabová, V.; Marek, M. *J. Phys. Chem.* **1994**, *98*, 3707.

(9) Hjelmfelt, A.; Schneider, F. W.; Ross, J. *Science* **1993**, *260*, 335. Hjelmfelt, A.; Ross, J. *J. Phys. Chem.* **1993**, *97*, 7988.

(10) Laplante, J.-P.; Pemberton, M.; Hjelmfelt, A.; Ross, J. *J. Phys. Chem.* **1995**, *99*, 10063.

(11) Dechert, G.; Zeyer, K.-P.; Lebender, D.; Schneider, F. W. *J. Phys. Chem.* **1996**, *100*, 19043.

(12) Hopfield, J. J. *Proc. Natl. Acad. Sci. U.S.A.* **1982**, *79*, 2554; *Proc. Natl. Acad. Sci. U.S.A.* **1984**, *81*, 3088.

(13) Pyragas, K. *Phys. Lett.* **1992**, *170A*, 421; *Z. Naturforsch.* **1993**, *48A*, 629.

(14) Noszticzius, Z.; Wittmann, M.; Stirling, P. *J. Phys. Chem.* **1985**, *89*, 4914. Noszticzius, Z.; Wittmann, M.; Stirling, P. *J. Chem. Phys.* **1987**, *86*, 1922.

(15) Dechert, G.; Lebender, D.; Schneider, F. W. *J. Phys. Chem.* **1995**, *99*, 11432.

(16) Györgyi, L.; Field, R. J. *J. Phys. Chem.* **1991**, *95*, 6594. Györgyi, L.; Field, R. J. *Nature* **1992**, *355*, 808.

(17) Gear, C. W. *Numerical Initial Value Problems in Ordinary Differential Equations*; Prentice Hall: Englewood Cliffs, NJ, 1971. Shampine, L. F.; Gear, C. W. *SIAM Rev.* **1979**, *21*, 1.